

Q-DiT: ACCURATE POST-TRAINING QUANTIZATION FOR DIFFUSION TRANSFORMERS

Lei Chen¹ Yuan Meng¹ Chen Tang¹ Xinzhu Ma² Jingyan Jiang³ Xin Wang¹ Zhi Wang¹ Wenwu Zhu¹
¹Tsinghua University ²MMLab, CUHK ³Shenzhen Technology University
 1-chen23@mails.tsinghua.edu.cn wangzhi@sz.tsinghua.edu.cn
 {yuanmeng, wwzhu}@tsinghua.edu.cn



Figure 1: Samples generated by GPTQ and Q-DiT with W4A8 on ImageNet 256×256 (Top) and ImageNet 512×512 (Bottom).

ABSTRACT

Recent advancements in diffusion models, particularly the trend of architectural transformation from UNet-based Diffusion to Diffusion Transformer (DiT), have significantly improved the quality and scalability of image synthesis. Despite the incredible generative quality, the large computational requirements of these large-scale models significantly hinder the deployments in real-world scenarios. Post-training Quantization (PTQ) offers a promising solution by compressing model sizes and speeding up inference for the pretrained models while eliminating model retraining. However, we have observed the existing PTQ frameworks exclusively designed for both ViT and conventional Diffusion models fall into biased quantization and result in remarkable performance degradation. In this paper, we find that the DiTs typically exhibit considerable variance in terms of both weight and activation, which easily runs out of the limited numerical representations. To address this issue, we devise Q-DiT, which seamlessly integrates three techniques: fine-grained quantization to manage substantial variance across input channels of

weights and activations, an automatic search strategy to optimize the quantization granularity and mitigate redundancies, and dynamic activation quantization to capture the activation changes across timesteps. Extensive experiments on the ImageNet dataset demonstrate the effectiveness of the proposed Q-DiT. Specifically, when quantizing DiT-XL/2 to W8A8 on ImageNet 256x256, Q-DiT achieves a remarkable reduction in FID by 1.26 compared to the baseline. Under a W4A8 setting, it maintains high fidelity in image generation, showcasing only a marginal increase in FID and setting a new benchmark for efficient, high-quality quantization in diffusion transformers. Code is available at <https://github.com/Juanerx/Q-DiT>.

1 INTRODUCTION

Diffusion models (Ho et al., 2020; Sohl-Dickstein et al., 2015; Song & Ermon, 2019; Song et al., 2020) have emerged as a powerful framework for generative tasks, revolutionized in various domains, ranging from computer vision (Rombach et al., 2022; Ruiz et al., 2023; Gal et al., 2022; Brempong et al., 2022), natural language processing (Austin et al., 2021; Hoogeboom et al., 2021) to multi-modal modeling (Avrahami et al., 2022; Ramesh et al., 2022). The architectural design of diffusion models has also undergone significant evolution. Traditionally, these models employed U-Net (Ronneberger et al., 2015) architectures due to their efficiency in handling hierarchical data representations (Ho et al., 2020; Rombach et al., 2022). However, recent advancements have seen a shift towards diffusion transformers (DiTs) (Peebles & Xie, 2023). Notable examples include Stable Diffusion 3 (Esser et al., 2024) and Sora (Brooks et al., 2024), which have demonstrated superior performance and scalability in complex generative tasks. The transition to transformer architectures is driven by their ability to capture long-range dependencies and their scalability to larger datasets and model sizes (Vaswani et al., 2017; Dosovitskiy et al., 2020), thus enhancing the model’s capacity to generate high-fidelity outputs.

Despite their success, a critical limitation of diffusion models lies in their inherently slow inference speeds. The iterative denoising process, while effective, requires numerous sampling steps, making real-time or large-scale applications computationally intensive. Recent research has focused on various strategies to mitigate this issue, such as developing efficient samplers (Song et al., 2021; Lu et al., 2022; Watson et al., 2021) to reduce the number of required sampling steps, and model compression techniques like distillation (Song et al., 2023), pruning (Fang et al., 2024) and quantization (Shang et al., 2023; He et al., 2024; 2023) to streamline model performance.

Model quantization increases sampling speed by reducing the precision of weight and activations. Among various quantization techniques, Post-Training quantization (PTQ) is widely used for quantizing large models since it does not require retraining; it only needs a small portion of the training dataset to calibrate the quantization parameters. However, the application of quantization techniques to transformer-based diffusion models remains largely unexplored. Existing quantization method for diffusion models (Shang et al., 2023; He et al., 2024; 2023) mainly focus on Unet architecture and mostly uses reconstruction-based methods, which are hard to scale to larger models (Nagel et al., 2020; Li et al., 2021). Furthermore, in our analysis, the reconstruction methods attempt to optimize the rounding policy by minimizing the mean squared error (MSE) between the full precision model and the quantized model, which proves to be suboptimal for diffusion transformers.

By analyzing the distribution of weights and activations, we identified the main challenges of DiT quantization: significant variance across the input channels of weights and structured outliers in activations. To address these challenges, Q-DiT integrates a fine-grained group quantization strategy that constrains high-magnitude values at the group level. Additionally, activations vary with different timesteps, indicating that quantization parameters calibrated at specific timesteps may not generalize well across all timesteps. To address this variability, Q-DiT adopts a dynamic activation quantization mechanism, which adapts to the changing distribution of activations throughout the diffusion process. This approach significantly reduces quantization error by adjusting quantization parameters on-the-fly, thus ensuring high-quality image generation with minimal overhead.

Moreover, we discovered redundancy in group sizes. Reducing group size does not always lead to better quantization performance. Consequently, Q-DiT employs an evolutionary search algorithm to optimally configure group sizes for quantization across different model layers. This method utilizes the Fréchet Inception Distance (FID) as a metric to directly correlate the quantization effects with

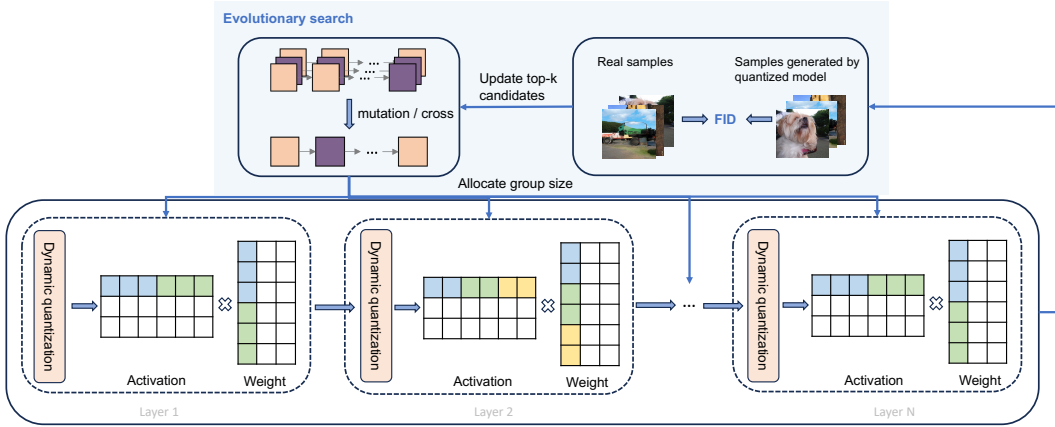


Figure 2: An overview of the proposed Q-DiT framework. The weights and activations within each layer are quantized with the same group size. The activations are dynamically quantized during runtime. Group size configurations allocated for each layer are based on the evolutionary search results, which are guided by the FID score between the real samples and samples generated by the quantized model.

the visual quality of generated images, enabling a more targeted and effective quantization strategy. The evolutionary approach not only identifies the most suitable group sizes but also ensures that the quantization process adheres to predefined computational constraints, thereby balancing performance with efficiency.

In summary, our main contributions are as follows:

- We introduce Q-DiT, an accurate post-training quantization scheme designed for diffusion transformers. This method employs fine-grained group quantization to effectively manage input channel variance in both weights and activations and adopts dynamic activation quantization to adapt to activation variations across different timesteps.
- We identified that the default group size configuration is suboptimal and propose an evolutionary search strategy to optimize group size allocation. This approach enhances the efficiency and efficacy of the quantization process.
- Extensive experiments on ImageNet demonstrate that Q-DiT achieves lossless compression under a W8A8 configuration and minimal degradation under W4A8 for image generation, showcasing its superior performance.

2 RELATED WORK

Model quantization. Model quantization is a widely used technique to reduce the size of a model and accelerate its inference speed by converting the model’s weights and activations from high-precision floating-point numbers to lower-precision numbers. Quantization can be approached in two main ways: Quantization-Aware Training (QAT) (Choi et al., 2018; Esser et al., 2019; Bhalgat et al., 2020) and Post-Training Quantization (PTQ) (Nagel et al., 2020; Li et al., 2021). QAT integrates the quantization process directly into the fine-tuning phase, leveraging STE (Bengio et al., 2013) to simultaneously optimize quantizer parameters and model parameters during fine-tuning. This approach restores the model’s performance degradation caused by quantization. However, QAT is rather costly, as it requires fine-tuning the model on the original training dataset. On the other hand, PTQ is much for efficient and useful because it doesn’t require retraining the model. This method works by using a small calibration dataset to adjust the quantization parameters for weights and activations, enabling significant model compression with minimal effort. Although PTQ is highly efficient, it can result in significant performance degradation when applied to low-bit quantization. Reconstruction-based method (Nagel et al., 2020; Li et al., 2021) tries to minimize performance degradation by reducing the reconstruction error of each layer or each block. Although the reconstruction-based method performs well in CNN, they are not easy to scale up to a large model.

Quantization of diffusion models. Diffusion models tend to have a slow inference speed due to the large number of sampling steps required. Consequently, some recent studies have focused on accelerating these models through quantization techniques. PTQ4DM (Shang et al., 2023) and Q-diffusion (Li et al., 2023a) discover activation variance across different denoising steps and adopt reconstruction-based methods for quantization. PTQD (He et al., 2024) finds the correlation between the quantization noise and model output and proposes variance schedule calibration to rectify the uncorrelated part. TDQ (So et al., 2024) utilizes an MLP layer to estimate the activation quantization parameters for each step. TMPQ-DM (Sun et al., 2024) further reduces the sequence length of timestep along with the quantization to reduce the overall costs. However, these methods are all designed for the Unet-based diffusion model and do not perform well in diffusion transformers, and we have observed that directly applying them to DiTs could a considerable performance drop.

Quantization of transformers. Quantization of transformers has been extensively researched in the contexts of both Vision Transformers (ViTs) and Large Language Models (LLMs). PTQ4ViT (Yuan et al., 2022) proposed the twin uniform quantizer to handle the special distributions of post-softmax and post-GELU activations. RepQ-ViT (Li et al., 2023b) used scale reparameterization to reduce the quantization error of activations. For LLM, weight-only quantization quantizes the weight to reduce the heavy memory movements to achieve better inference efficiency. GPTQ (Frantar et al., 2022) reduced the bit-width to 4 bits per weight based on approximate second-order information with weight-only quantization. AWQ (Lin et al., 2023) proposed activation-aware weight quantization to reduce the quantization error of salient weight. On the other hand, weight-activation quantization further enhances inference efficiency by quantizing both weight and activation but has to face activation outliers. LLM.int8() (Dettmers et al., 2022) reduces the effect of outliers by keeping them in FP16 with mixed-precision computations. Outlier Suppression (Wei et al., 2022) reduces the quantization error of activations by using the non-scaling LayerNorm. However, the quantization techniques may not be directly applied to DiTs, due to their diffusion model characteristics.

3 Q-DiT

3.1 PRELIMINARY

We adopt uniform quantization to quantize both weights and activations in our experiments since it is more hardware friendly (Jacob et al., 2018; Han et al., 2015). Uniform quantization divides the range of floating-point values into equally spaced intervals, and each interval is mapped to a discrete value. The uniform quantization function that quantize input floating point value x into b bit integer can be expressed as:

$$\hat{x} = Q_b(x, s) = s \cdot (\text{clip}(\lfloor \frac{x}{s} \rfloor + Z, 0, 2^b - 1) - Z), \quad (1)$$

where $s = \frac{\max(x) - \min(x)}{2^b - 1}$, $Z = -\lfloor \frac{\min(x)}{s} \rfloor$. Here, $\lfloor \cdot \rfloor$ is the round operation, s is the scaling factor and Z denotes the zero point.

3.2 REQUIREMENTS OF FINE-GRAINED QUANTIZATION

We have observed that directly applying recent UNet-based quantization methods to quantize DiT results in significant performance degradation, as shown in Tab. 2 and Tab. 3. This is primarily because these works focused on optimizing for UNet architecture with the basic operator of convolutional neural networks (CNNs). In this section, we first identify the challenges of DiT quantization by analyzing the distribution of both weights and activations and then propose a fine-grained group quantization method to address this issue.

Observation 1: DiTs exhibit significant variance across input channels of weights. As shown in Fig. 3a, the variance across input channels of weight is much more significant than the output channels, which substantially affects quantization, as a common quantization scheme applies channel-wise quantization along the output channel. We hypothesize that this is because the *input channels of the weights handle the correlations between different features of all input tokens, whereas the output channels deal with the information of the same feature across different tokens*. The variance between different features is larger than the variance within the same feature across different tokens, making

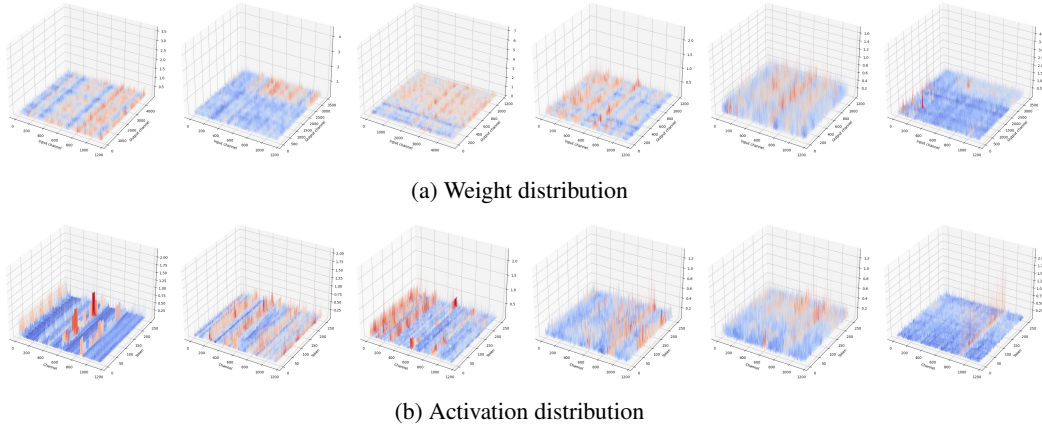


Figure 3: The distribution of weight and activation of different layers. For weight distribution, the variance across input channels is more dominant than the variance across output channels. For activation distribution, outliers in specific channels pose great challenges for per-tensor quantization.

the input channels more critical. Therefore, we propose to quantize the weights along with the input channels based on this observation.

Observation②: Structured outliers in activations. The outliers persist in specific channels of the activation as shown in Fig. 3b. This suggests that, if we still use tensor-wise quantization, these outliers significantly impact the quantization parameters, resulting in substantial quantization errors for these non-outliers.

One simple solution is to apply input channel-wise quantization for both the weights and activation, using different quantization parameters for each channel. However, this scheme leads to decreased computational efficiency during hardware deployment, as we cannot leverage the low-precision computation anymore (Bondarenko et al., 2021; Xiao et al., 2023). Inspired by recent work on large language model (LLM) quantization (Lin et al., 2023; Zhao et al., 2024), we adopt group quantization to reduce quantization error without sacrificing much computational efficiency. As depicted in Fig. 2, each weight and activation matrix are divided into groups, and we perform quantization for each group separately.

3.3 DYNAMIC ACTIVATION QUANTIZATION

Observation③: Distribution shift of activations across timesteps. We have further observed that the distribution of activations in DiT models undergoes significant changes at different timesteps during the denoising process, as demonstrated in Fig. 4 and Fig. 5. In UNet-based diffusion quantization, previous studies have either allocated a set of quantization parameters for all activations at each timestep (He et al., 2023) or designed a multi-layer perceptron (MLP) (So et al., 2024) to predict quantization parameters based on the timestep. However, these methods are not compatible with our fine-grained quantization because assigning quantization parameters to each group at every timestep results in considerable memory overheads.

Inspired by the recent advances in LLM optimization (Wu et al., 2023), we adopt an on-the-fly dynamic quantization approach for activations. Specifically, during inference, the quantization parameters for each group of the activations are calculated based on their min-max values. Furthermore, we fuse the dynamic quantization with min-max computation into the prior operator (e.g., linear projections), which can benefit from the operator fusion and the overhead becomes negligible compared to the costly matrix multiplications in transformer blocks.

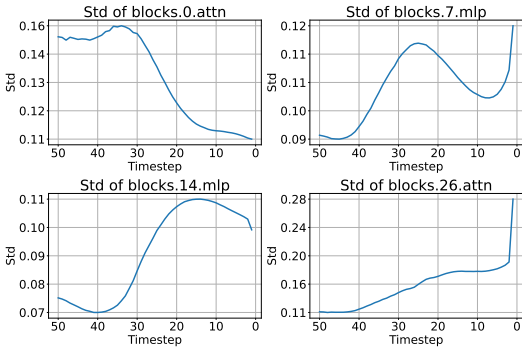


Figure 4: Standard deviation of activation across different 50 timesteps of DiT-XL/2 on ImageNet 256 × 256 .

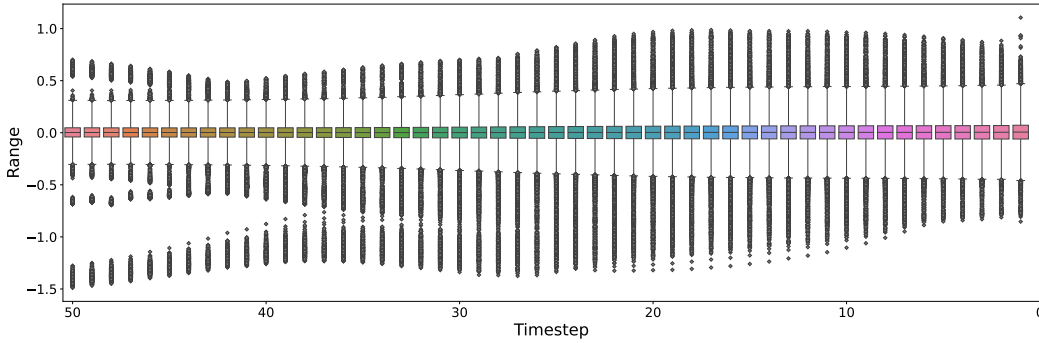


Figure 5: Distribution of activation across different timesteps of DiT-XL/2 on ImageNet 256×256 .

3.4 AUTOMATIC QUANTIZATION GRANULARITY ALLOCATION

Observation 4: Non-monotonicity in quantization group selection. Ideally, we can improve model performance by reducing the group size since finer-grained quantization reduces quantization error, as demonstrated in previous LLM quantization research [Frantar et al. \(2022\)](#).

However, as shown in Tab. 1, we have observed that smaller group sizes do not always yield better results, where such existence of non-monotonicity in the quantization group further demonstrates that DiT quantization is rather different compared with the Large Language Model and Vision-Transformer. For instance, when the group size was reduced from 128 to 96, the FID increased by about 11.8%, from 17.87 to 19.97, indicating a degradation in the quality of generated images.

256×256			512×512		
Group	FID	sFID	Group	FID	sFID
128	17.87	20.45	96	20.76	21.97
96	19.97	21.42	64	20.90	22.58

Table 1: Quantization results with varying group sizes on ImageNet 256×256 and 512×512 .

This suggests that there is an optimal group size configuration that can achieve better quantization effects with the same average group size or achieve the same quantization effect with a larger average group size. Additionally, the sensitivity of each layer in the model varies. By assigning different group sizes to different layers, we can achieve high efficiency and quality in both model performance and image generation.

Automatic group allocation. The primary challenge in allocating group sizes lies in identifying the correlation between the group size of each layer and the final task loss of the diffusion model. Previous work on mixed precision has focused on identifying sensitivity indicators ([Li et al., 2021](#); [Tang et al., 2022](#)) for each layer, such as the mean squared error (MSE) between the quantized layer and the full precision layer, and then transforming this into an integer linear programming (ILP) problem for optimization. However, we found that a smaller MSE does not necessarily correspond to a smaller final task loss. This discrepancy may be due to the iterative denoising process inherent in diffusion models.

To address this, we use the FID between samples generated by the quantized model and the real samples as our metric as follows:

$$L(\hat{\mathbf{w}}, \mathbf{g}) = \text{FID}(R, G_{\hat{\mathbf{w}}, \mathbf{g}}) \tag{2}$$

where $\hat{\mathbf{w}}$ is the quantized weight, and \mathbf{g} is the group size configuration for each layer. R and $G_{\hat{\mathbf{w}}, \mathbf{g}}$ denote the real images and the images generated by the quantized model, respectively. We then employ an evolutionary algorithm to optimize the following objective function:

$$\mathbf{g}^* = \arg \min_{\mathbf{g}} L(\hat{\mathbf{w}}, \mathbf{g}), \quad \text{s.t. } B(\mathbf{g}) \leq N_{bitops}, \tag{3}$$

Here $B(\cdot)$ is the measurement of bit-operations (BitOps) and N_{bitops} is the predefined threshold.

This approach allows us to better capture the nuanced impacts of group size on model performance, leading to improved outcomes in both efficiency and image quality. The algorithm is located in Alg. 1.

4 EXPERIMENTS

4.1 SETTINGS

Models and dataset. The evaluation settings closely follow those in the original DiT paper (Peebles & Xie, 2023). We used the pre-trained DiT-XL/2 models with image resolutions of 256×256 and 512×512 , converting them to FP16 for efficient inference. The quantized models were evaluated on ImageNet (Deng et al., 2009) datasets at both 256×256 and 512×512 resolutions. For fast and accurate sampling, we adopted the DDIM sampler (Song et al., 2021) with 50 and 100 sampling steps. Performance was also evaluated with and without classifier-free guidance (Ho & Salimans, 2021) to verify the robustness of our proposed method. Note that "cfg" denotes the classifier-free guidance scale.

Metrics. To evaluate the generation quality of the quantized model, we followed previous literature and employed four metrics: Fréchet Inception Distance (FID) (Heusel et al., 2017), spatial FID (sFID) (Salimans et al., 2016), Inception Score (IS), and Precision. All metrics were computed using ADM’s TensorFlow evaluation suite (Dhariwal & Nichol, 2021). For both ImageNet 256×256 and ImageNet 512×512 , we sampled 10k images for evaluation.

Quantization. Q-DiT uses asymmetric quantization for both weights and activations and applied GPTQ (Frantar et al., 2022) for weight quantization. We adopted the MinMax quantization technique due to its simplicity and effectiveness. A default group size of 128 was used, and a better group size allocation for each layer was found through evolutionary search. The search space for group size was $\{32, 64, 128, 192, 288\}$, with a target group size of 128. Note that the group size for weights and activations in the same layer should be the same.

Baselines. We compared Q-DiT with three strong baselines: PTQ4DM (Shang et al., 2023), RepQ-ViT (Li et al., 2023b), and GPTQ (Frantar et al., 2022), which are advanced post-training quantization techniques for diffusion models, ViTs, and LLMs respectively. The original GPTQ is a weight-only quantization method. To transform it into a comparable weight-activation quantization, we employed the same method used in PTQ4DM to quantize the activations.

4.2 MAIN RESULTS

Our experimental evaluation focused on the quantization of DiT-XL/2 model on ImageNet 256×256 and ImageNet 512×512 dataset, employing different timesteps and classifier-free guidance settings. The quantitative results are presented in Tab. 2 and 3. Specifically, the PTQ4DM method demonstrated substantial performance degradation at a bit-width of W8A8, resulting in a FID increase from 12.40 in FP to 20.91, and a reduction in IS from 116.68 to 81.72. Contrastingly, RepQ-ViT, GPTQ, and Q-DiT exhibited notable improvements over PTQ4DM in the W8A8 setting. RepQ-ViT improved the FID to 13.19 and the IS to 113.35, signifying a marked enhancement in maintaining the quality and diversity of generated images. Our approach further minimized the quantization impact, closely matching the FP configuration with an FID of 11.93 and an IS of 119.86. This result underscores our method’s effectiveness in achieving near-lossless compression in the 8/8 quantization setting.

Algorithm 1: Automatic quantization granularity allocation of Q-DiT

Input: population size N_p ; iterations N_{iter} ; mutation probability p ; Constraint

```

 $N_{bitops}$ 
Initialize  $N_p$  group size configuration
candidates;
Initialize  $TopK$  candidates;
for  $t = 1, 2, \dots, N_{iter}$  do
    Quantize each candidate using its group
    configuration and generate images;
    Evaluate FID for each candidate based on
    equation 2;
    Update  $TopK$  candidate based on the FID
    score;
    repeat
        New candidate  $\mathbf{g}$  by crossover if
         $B(\mathbf{g}) < N_{bitops}$ ;
    until Size of  $N_{cross}$  equal to  $N_p/2$ ;
    repeat
        New candidate  $\mathbf{g}$  by mutation if
         $B(\mathbf{g}) < N_{bitops}$ ;
    until Size of  $N_{mutation}$  equal to  $N_p/2$ ;
Get the best group configuration and quantize
the model;
return quantized model

```

Table 2: Quantitative results of quantizing DiT-XL/2 on ImageNet 256×256. ‘W/A’ indicates the bit-width of weight and activation, respectively.

Model	Bit-width (W/A)	Method	Size (MB)	FID ↓	sFID ↓	IS ↑	Precision ↑	
DiT-XL/2 (steps = 100)	16/16	FP	1349	12.40	19.11	116.68	0.6605	
	8/8	PTQ4DM	677	20.91	22.50	81.72	0.5714	
		RepQ-ViT	677	13.19	20.31	113.35	0.6523	
		GPTQ	690	16.44	23.51	102.10	0.6149	
		Ours	683	11.93	18.18	119.86	0.6683	
	4/8	PTQ4DM	339	252.31	82.44	2.74	0.0125	
		RepQ-ViT	339	315.85	139.99	2.11	0.0067	
		GPTQ	351	25.48	25.57	73.46	0.5392	
		Ours	347	15.76	19.84	98.78	0.6395	
	DiT-XL/2 (steps = 100 cfg = 1.5)	16/16	FP	1349	5.31	17.61	245.85	0.8077
		8/8	PTQ4DM	677	10.81	24.50	158.73	0.6699
			RepQ-ViT	677	5.27	17.99	241.51	0.7986
GPTQ			690	6.01	19.02	227.58	0.7726	
Ours			683	5.34	17.47	243.94	0.8063	
4/8		PTQ4DM	339	255.06	84.63	2.76	0.011	
		RepQ-ViT	339	311.31	138.58	2.18	0.072	
		GPTQ	351	7.66	20.76	193.76	0.7261	
		Ours	347	6.40	18.60	211.72	0.7609	
DiT-XL/2 (steps = 50)		16/16	FP	1349	13.47	19.31	114.71	0.6601
		8/8	PTQ4DM	677	30.63	26.43	58.81	0.4947
			RepQ-ViT	677	14.28	20.65	111.62	0.6479
	GPTQ		690	17.17	23.62	98.15	0.6130	
	Ours		683	13.09	18.30	115.80	0.6686	
	4/8	PTQ4DM	339	256.15	83.45	2.73	0.015	
		RepQ-ViT	339	324.25	142.98	2.12	0.0062	
		GPTQ	351	26.31	25.54	69.73	0.5388	
		Ours	347	17.42	19.95	97.52	0.6219	
	DiT-XL/2 (steps = 50 cfg = 1.5)	16/16	FP	1349	5.32	17.64	236.17	0.8040
		8/8	PTQ4DM	677	7.99	22.98	184.79	0.7185
			RepQ-ViT	677	5.46	18.11	234.74	0.7968
GPTQ			690	5.90	19.60	218.90	0.7772	
Ours			683	5.45	17.57	236.52	0.8091	
4/8		PTQ4DM	339	261.76	95.27	2.39	0.0084	
		RepQ-ViT	339	319.68	141.68	2.20	0.0068	
		GPTQ	351	9.94	21.79	166.35	0.6906	
		Ours	347	6.75	18.27	208.38	0.7673	

When the bit-width was reduced to W4A8, the performance disparities among the methods became more pronounced. Both PTQ4DM and RepQ-ViT experience significant degradation in performance, with PTQ4DM reaching an FID of 252.31 and RepQ-ViT an FID of 315.85, while IS plummeted to 2.74 and 2.11, respectively. GPTQ performs better than these two methods, as it provides a more advanced technique for quantizing the weight of transformers. In contrast, our method substantially outperformed these baselines, dramatically reducing quantization loss with an FID of 16.76 and an IS of 96.78. This demonstrates a significant preservation of quality and diversity at lower bit-widths, highlighting the robustness of our approach under stringent quantization constraints.

Across varying steps (100 and 50) and classifier free guidance scales, our method consistently showed superior performance, closely emulating the full-precision model metrics. The evaluation on the ImageNet 512×512 dataset, detailed in Tab. 3, showed consistent trends with the 256×256 dataset, which demonstrate that Q-DiT can also perform well to high-resolution image generation. The visual demonstrations are shown in Fig. 1 to further illustrate the effectiveness of our method.

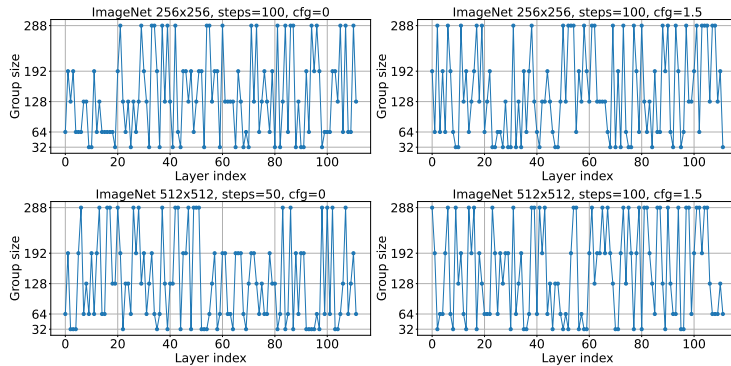
4.3 ABLATION STUDIES

Visualization. The group size configurations for different models are shown in Fig. 6.

Table 3: Quantitative results of quantizing DiT-XL/2 on ImageNet 512×512. ‘W/A’ indicates the bit-width of weight and activation, respectively.

Model	Bit-width (W/A)	Method	Size (MB)	FID ↓	sFID ↓	IS ↑	Precision ↑	
DiT-XL/2 (steps = 50)	16/16	FP	1349	16.01	20.50	97.79	0.7481	
	8/8	PTQ4DM	677	18.58	23.67	94.10	0.7426	
		RepQ-ViT	677	16.01	20.48	97.10	0.7458	
		GPTQ	690	17.51	21.00	96.08	0.7471	
		Ours	683	16.23	20.75	96.73	0.7454	
	4/8	PTQ4DM	339	131.66	75.79	11.54	0.1847	
		RepQ-ViT	339	105.32	65.63	18.01	0.2504	
		GPTQ	351	26.58	24.14	70.24	0.6655	
		Ours	348	21.59	22.26	81.80	0.7076	
	DiT-XL/2 (steps = 50 cfg = 1.5)	16/16	FP	1349	6.27	18.45	204.47	0.8343
		8/8	PTQ4DM	677	7.41	22.06	178.33	0.7541
			RepQ-ViT	677	6.18	18.39	202.76	0.8352
GPTQ			690	7.11	19.49	194.46	0.8406	
Ours			683	6.28	18.54	203.31	0.8345	
4/8		PTQ4DM	339	88.45	50.80	26.79	0.3206	
		RepQ-ViT	339	79.69	49.76	29.46	0.3413	
		GPTQ	351	9.98	20.76	156.07	0.7840	
		Ours	347	7.82	19.60	174.18	0.8127	

We have observed that for different models (e.g., different generation resolutions, different cfg scales), the optimal grouping strategies are quite different, e.g., for higher generation resolution, the top layers have larger group sizes, while for lower generation resolution, the middle layers exhibit the requirements of larger group sizes.



Effectiveness of the proposed method.

To evaluate the effectiveness of each proposed component, we conducted a comprehensive ablation study on ImageNet 256×256. This analysis employed the DiT-XL/2 model with a DDIM sampler, setting the sampling steps to 100 and the classifier-free guidance scale to 1.5, as detailed in Tab. 4. We began our assessment with a baseline round-to-nearest (RTN) method, which simply rounds weights and activations to the nearest available quantization level. Under the W4A8 configuration, RTN demonstrated significantly low performance across all metrics, highlighting the limitations of aggressive quantization. Enhancing RTN by adjusting the quantization granularity to a group size

Figure 6: Group size configuration for models at different resolutions, steps and cfg scales.

Table 4: The effect of different components proposed in the paper. The experiment is conducted over DiT-XL/2 on ImageNet 256 × 256 with cfg=1.5 and steps=100.

Method	Bit-width (W/A)	FID↓	sFID↓	IS↑	Precision↑
FP16	16/16	5.31	17.61	242.68	0.8076
RTN	4/8	225.50	88.54	2.96	0.0676
+ Group size 128	4/8	13.77	27.41	146.93	0.6412
+ Dynamic activation quantization	4/8	6.64	19.29	211.27	0.7548
+ Group size allocation	4/8	6.40	18.60	211.72	0.7609

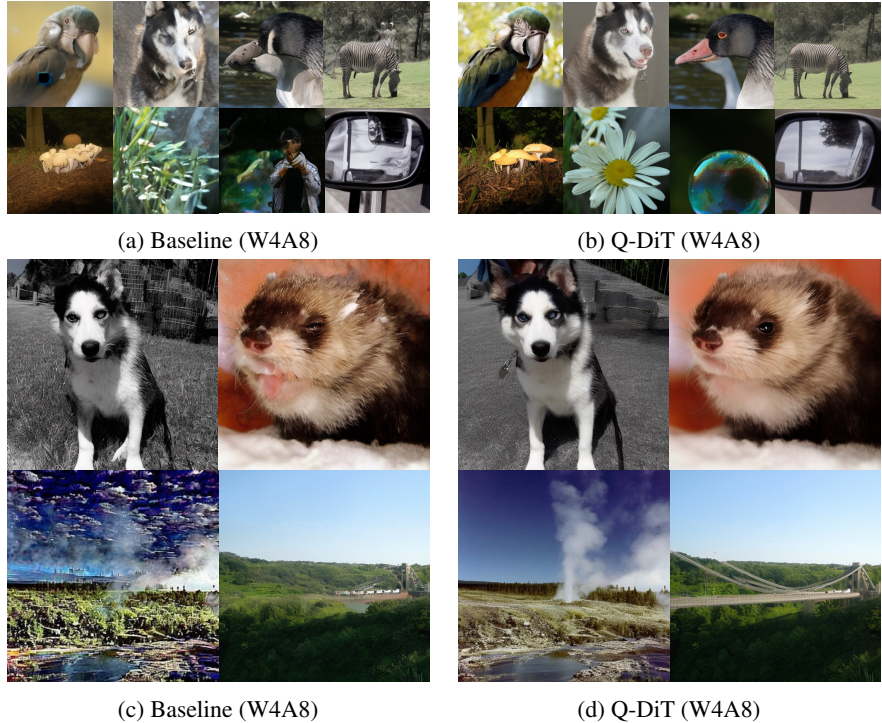


Figure 7: Samples generated by GPTQ and Q-DiT with W4A8 on ImageNet 256×256 (Top) and ImageNet 512×512 (Bottom).

Table 5: The effect of the proposed search method compared to others. The experiment is conducted over DiT-XL/2 on ImageNet 256 × 256 with cfg=1.5 and steps=100.

Method	Bit-width (W/A)	FID↓	sFID↓	IS↑	Precision↑
Group size = 128	4/8	6.64	19.29	211.27	0.7548
Integer Linear Programming	4/8	6.71	19.20	205.54	0.7538
Hessian-based	4/8	7.38	19.41	197.48	0.7385
Ours	4/8	6.40	18.60	211.72	0.7609

of 128 markedly improved the results. The introduction of dynamic activation quantization led to a significant boost in generation quality, evidenced by an FID of 6.64, an sFID of 18.29, and an IS of 211.27. By further incorporating group size allocation, our approach achieved an impressive FID of 6.40, approaching the performance of the full-precision model.

The effectiveness of our search method was also compared with the ILP method (Moon et al., 2024) and the Hessian-based search method (Li et al., 2021). As presented in Tab. 5, ILP and Hessian-based methods achieved FIDs of 6.71 and 7.38, respectively, both greater than the FID achieved with our default group size of 128. In contrast, our proposed method reduced the FID by 0.24, showcasing its efficacy.

5 CONCLUSION

Our study presents Q-DiT, a novel post-training quantization framework specifically designed for diffusion transformers, which has demonstrated robust performance in image generation tasks with minimal quality degradation. To address the significant variance in input channels for weights and

activations, we introduced group quantization. Furthermore, to manage variations in activation ranges across different timesteps, we implemented dynamic activation quantization that adaptively adjusts quantization parameters during runtime. Additionally, to resolve issues of group redundancy, we employed an evolutionary search algorithm to optimize the grouping strategy. Extensive experiments have underscored the effectiveness of our approach, showcasing its superiority over existing baselines. Notably, even when quantizing the model to W4A8 on the ImageNet 256×256 dataset, the FID increased by only 1.29, demonstrating our method’s efficiency in maintaining high image quality under stringent quantization constraints.

Limitations and future work. One of the primary limitations of the current Q-DiT approach is its reliance on evolutionary algorithms to determine the optimal group size configurations for quantization. While evolutionary algorithms are versatile in navigating complex search spaces, they require substantial computational resources, particularly due to the necessity of computing the FID for assessing model performance. This evaluation metric, although effective in measuring the quality of images generated by models, is computationally expensive and time-consuming, which increases the overall cost and duration of the optimization process. Additionally, the current implementation of Q-DiT has been primarily tested on the ImageNet dataset. To broaden the applicability and robustness of our approach, future studies will aim to extend the experimentation to other domains such as text-to-image generation and video generation.

REFERENCES

- Jacob Austin, Daniel D Johnson, Jonathan Ho, Daniel Tarlow, and Rianne Van Den Berg. Structured denoising diffusion models in discrete state-spaces. *Advances in Neural Information Processing Systems*, 34:17981–17993, 2021.
- Omri Avrahami, Dani Lischinski, and Ohad Fried. Blended diffusion for text-driven editing of natural images. In *Proceedings of the IEEE/CVF Conference on Computer Vision and Pattern Recognition*, pp. 18208–18218, 2022.
- Yoshua Bengio, Nicholas Léonard, and Aaron Courville. Estimating or propagating gradients through stochastic neurons for conditional computation. *arXiv preprint arXiv:1308.3432*, 2013.
- Yash Bhalgat, Jinwon Lee, Markus Nagel, Tijmen Blankevoort, and Nojun Kwak. Lsq+: Improving low-bit quantization through learnable offsets and better initialization. In *Proceedings of the IEEE/CVF conference on computer vision and pattern recognition workshops*, pp. 696–697, 2020.
- Yelysei Bondarenko, Markus Nagel, and Tijmen Blankevoort. Understanding and overcoming the challenges of efficient transformer quantization. *arXiv preprint arXiv:2109.12948*, 2021.
- Emmanuel Asiedu Brempong, Simon Kornblith, Ting Chen, Niki Parmar, Matthias Minderer, and Mohammad Norouzi. Denoising pretraining for semantic segmentation. In *Proceedings of the IEEE/CVF conference on computer vision and pattern recognition*, pp. 4175–4186, 2022.
- Tim Brooks, Bill Peebles, Connor Holmes, Will DePue, Yufei Guo, Li Jing, David Schnurr, Joe Taylor, Troy Luhman, Eric Luhman, Clarence Ng, Ricky Wang, and Aditya Ramesh. Video generation models as world simulators. 2024. URL <https://openai.com/research/video-generation-models-as-world-simulators>.
- Jungwook Choi, Zhuo Wang, Swagath Venkataramani, Pierce I-Jen Chuang, Vijayalakshmi Srinivasan, and Kailash Gopalakrishnan. Pact: Parameterized clipping activation for quantized neural networks. *arXiv preprint arXiv:1805.06085*, 2018.
- Jia Deng, Wei Dong, Richard Socher, Li-Jia Li, Kai Li, and Li Fei-Fei. Imagenet: A large-scale hierarchical image database. In *CVPR*, 2009.
- Tim Dettmers, Mike Lewis, Younes Belkada, and Luke Zettlemoyer. Gpt3. int8 (): 8-bit matrix multiplication for transformers at scale. *Advances in Neural Information Processing Systems*, 35: 30318–30332, 2022.
- Prafulla Dhariwal and Alexander Nichol. Diffusion models beat gans on image synthesis. In *NeurIPS*, volume 34, pp. 8780–8794, 2021.

- Alexey Dosovitskiy, Lucas Beyer, Alexander Kolesnikov, Dirk Weissenborn, Xiaohua Zhai, Thomas Unterthiner, Mostafa Dehghani, Matthias Minderer, Georg Heigold, Sylvain Gelly, et al. An image is worth 16x16 words: Transformers for image recognition at scale. *arXiv preprint arXiv:2010.11929*, 2020.
- Patrick Esser, Sumith Kulal, Andreas Blattmann, Rahim Entezari, Jonas Müller, Harry Saini, Yam Levi, Dominik Lorenz, Axel Sauer, Frederic Boesel, et al. Scaling rectified flow transformers for high-resolution image synthesis. *arXiv preprint arXiv:2403.03206*, 2024.
- Steven K Esser, Jeffrey L McKinstry, Deepika Bablani, Rathinakumar Appuswamy, and Dharmendra S Modha. Learned step size quantization. *arXiv preprint arXiv:1902.08153*, 2019.
- Gongfan Fang, Xinyin Ma, and Xinchao Wang. Structural pruning for diffusion models. *Advances in neural information processing systems*, 36, 2024.
- Elias Frantar, Saleh Ashkboos, Torsten Hoefler, and Dan Alistarh. Gptq: Accurate post-training quantization for generative pre-trained transformers. *arXiv preprint arXiv:2210.17323*, 2022.
- Rinon Gal, Yuval Alaluf, Yuval Atzmon, Or Patashnik, Amit H Bermano, Gal Chechik, and Daniel Cohen-Or. An image is worth one word: Personalizing text-to-image generation using textual inversion. *arXiv preprint arXiv:2208.01618*, 2022.
- Song Han, Huizi Mao, and William J Dally. Deep compression: Compressing deep neural networks with pruning, trained quantization and huffman coding. *arXiv preprint arXiv:1510.00149*, 2015.
- Yefei He, Jing Liu, Weijia Wu, Hong Zhou, and Bohan Zhuang. Efficientdm: Efficient quantization-aware fine-tuning of low-bit diffusion models. *arXiv preprint arXiv:2310.03270*, 2023.
- Yefei He, Luping Liu, Jing Liu, Weijia Wu, Hong Zhou, and Bohan Zhuang. Ptqd: Accurate post-training quantization for diffusion models. *Advances in Neural Information Processing Systems*, 36, 2024.
- Martin Heusel, Hubert Ramsauer, Thomas Unterthiner, Bernhard Nessler, and Sepp Hochreiter. Gans trained by a two time-scale update rule converge to a local nash equilibrium. In *NeurIPS*, 2017.
- Jonathan Ho and Tim Salimans. Classifier-free diffusion guidance. In *NeurIPS 2021 Workshop on Deep Generative Models and Downstream Applications*, 2021.
- Jonathan Ho, Ajay Jain, and Pieter Abbeel. Denoising diffusion probabilistic models. *Advances in neural information processing systems*, 33:6840–6851, 2020.
- Emiel Hoogetboom, Didrik Nielsen, Priyank Jaini, Patrick Forré, and Max Welling. Argmax flows and multinomial diffusion: Learning categorical distributions. *Advances in Neural Information Processing Systems*, 34:12454–12465, 2021.
- Benoit Jacob, Skirmantas Kligys, Bo Chen, Menglong Zhu, Matthew Tang, Andrew Howard, Hartwig Adam, and Dmitry Kalenichenko. Quantization and training of neural networks for efficient integer-arithmetic-only inference. In *Proceedings of the IEEE conference on computer vision and pattern recognition*, pp. 2704–2713, 2018.
- Xiuyu Li, Yijiang Liu, Long Lian, Huanrui Yang, Zhen Dong, Daniel Kang, Shanghang Zhang, and Kurt Keutzer. Q-diffusion: Quantizing diffusion models. In *Proceedings of the IEEE/CVF International Conference on Computer Vision*, pp. 17535–17545, 2023a.
- Yuhang Li, Ruihao Gong, Xu Tan, Yang Yang, Peng Hu, Qi Zhang, Fengwei Yu, Wei Wang, and Shi Gu. Brecq: Pushing the limit of post-training quantization by block reconstruction. *arXiv preprint arXiv:2102.05426*, 2021.
- Zhikai Li, Junrui Xiao, Lianwei Yang, and Qingyi Gu. Repq-vit: Scale reparameterization for post-training quantization of vision transformers. In *Proceedings of the IEEE/CVF International Conference on Computer Vision*, pp. 17227–17236, 2023b.
- Ji Lin, Jiaming Tang, Haotian Tang, Shang Yang, Wei-Ming Chen, Wei-Chen Wang, Guangxuan Xiao, Xingyu Dang, Chuang Gan, and Song Han. Awq: Activation-aware weight quantization for llm compression and acceleration. *arXiv preprint arXiv:2306.00978*, 2023.

- Cheng Lu, Yuhao Zhou, Fan Bao, Jianfei Chen, Chongxuan Li, and Jun Zhu. Dpm-solver: A fast ode solver for diffusion probabilistic model sampling in around 10 steps. *Advances in Neural Information Processing Systems*, 35:5775–5787, 2022.
- Jaehyeon Moon, Dohyung Kim, Junyong Cheon, and Bumsu Ham. Instance-aware group quantization for vision transformers. In *Proceedings of the IEEE/CVF Conference on Computer Vision and Pattern Recognition*, pp. 16132–16141, 2024.
- Markus Nagel, Rana Ali Amjad, Mart Van Baalen, Christos Louizos, and Tijmen Blankevoort. Up or down? adaptive rounding for post-training quantization. In *International Conference on Machine Learning*, pp. 7197–7206. PMLR, 2020.
- William Peebles and Saining Xie. Scalable diffusion models with transformers. In *Proceedings of the IEEE/CVF International Conference on Computer Vision*, pp. 4195–4205, 2023.
- Aditya Ramesh, Prafulla Dhariwal, Alex Nichol, Casey Chu, and Mark Chen. Hierarchical text-conditional image generation with clip latents. arXiv 2022. *arXiv preprint arXiv:2204.06125*, 2022.
- Robin Rombach, Andreas Blattmann, Dominik Lorenz, Patrick Esser, and Björn Ommer. High-resolution image synthesis with latent diffusion models. In *Proceedings of the IEEE/CVF conference on computer vision and pattern recognition*, pp. 10684–10695, 2022.
- Olaf Ronneberger, Philipp Fischer, and Thomas Brox. U-net: Convolutional networks for biomedical image segmentation. In *MICCAI*, pp. 234–241. Springer, 2015.
- Nataniel Ruiz, Yuanzhen Li, Varun Jampani, Yael Pritch, Michael Rubinstein, and Kfir Aberman. Dreambooth: Fine tuning text-to-image diffusion models for subject-driven generation. In *Proceedings of the IEEE/CVF Conference on Computer Vision and Pattern Recognition*, pp. 22500–22510, 2023.
- Tim Salimans, Ian Goodfellow, Wojciech Zaremba, Vicki Cheung, Alec Radford, and Xi Chen. Improved techniques for training gans. In *NeurIPS*, 2016.
- Yuzhang Shang, Zhihang Yuan, Bin Xie, Bingzhe Wu, and Yan Yan. Post-training quantization on diffusion models. In *CVPR*, 2023.
- Junhyuk So, Jungwon Lee, Daehyun Ahn, Hyungjun Kim, and Eunhyeok Park. Temporal dynamic quantization for diffusion models. *Advances in Neural Information Processing Systems*, 36, 2024.
- Jascha Sohl-Dickstein, Eric Weiss, Niru Maheswaranathan, and Surya Ganguli. Deep unsupervised learning using nonequilibrium thermodynamics. In *International conference on machine learning*, pp. 2256–2265. PMLR, 2015.
- Jiaming Song, Chenlin Meng, and Stefano Ermon. Denoising diffusion implicit models. In *ICLR*, 2021.
- Yang Song and Stefano Ermon. Generative modeling by estimating gradients of the data distribution. *Advances in neural information processing systems*, 32, 2019.
- Yang Song, Jascha Sohl-Dickstein, Diederik P Kingma, Abhishek Kumar, Stefano Ermon, and Ben Poole. Score-based generative modeling through stochastic differential equations. *arXiv preprint arXiv:2011.13456*, 2020.
- Yang Song, Prafulla Dhariwal, Mark Chen, and Ilya Sutskever. Consistency models. *arXiv preprint arXiv:2303.01469*, 2023.
- Haojun Sun, Chen Tang, Zhi Wang, Yuan Meng, Xinzhu Ma, Wenwu Zhu, et al. Tmpq-dm: Joint timestep reduction and quantization precision selection for efficient diffusion models. *arXiv preprint arXiv:2404.09532*, 2024.
- Chen Tang, Kai Ouyang, Zhi Wang, Yifei Zhu, Wen Ji, Yaowei Wang, and Wenwu Zhu. Mixed-precision neural network quantization via learned layer-wise importance. In *European Conference on Computer Vision*, pp. 259–275. Springer, 2022.

- Ashish Vaswani, Noam Shazeer, Niki Parmar, Jakob Uszkoreit, Llion Jones, Aidan N Gomez, Łukasz Kaiser, and Illia Polosukhin. Attention is all you need. *Advances in neural information processing systems*, 30, 2017.
- Daniel Watson, William Chan, Jonathan Ho, and Mohammad Norouzi. Learning fast samplers for diffusion models by differentiating through sample quality. In *International Conference on Learning Representations*, 2021.
- Xiuying Wei, Yunchen Zhang, Xiangguo Zhang, Ruihao Gong, Shanghang Zhang, Qi Zhang, Fengwei Yu, and Xianglong Liu. Outlier suppression: Pushing the limit of low-bit transformer language models. *Advances in Neural Information Processing Systems*, 35:17402–17414, 2022.
- Xiaoxia Wu, Zhewei Yao, and Yuxiong He. Zeroquant-fp: A leap forward in llms post-training w4a8 quantization using floating-point formats. *arXiv preprint arXiv:2307.09782*, 2023.
- Guangxuan Xiao, Ji Lin, Mickael Seznec, Hao Wu, Julien Demouth, and Song Han. SmoothQuant: Accurate and efficient post-training quantization for large language models. In *Proceedings of the 40th International Conference on Machine Learning*, 2023.
- Zhihang Yuan, Chenhao Xue, Yiqi Chen, Qiang Wu, and Guangyu Sun. Ptq4vit: Post-training quantization for vision transformers with twin uniform quantization. In *European conference on computer vision*, pp. 191–207. Springer, 2022.
- Yilong Zhao, Chien-Yu Lin, Kan Zhu, Zihao Ye, Lequn Chen, Size Zheng, Luis Ceze, Arvind Krishnamurthy, Tianqi Chen, and Baris Kasikci. Atom: Low-bit quantization for efficient and accurate llm serving. *Proceedings of Machine Learning and Systems*, 6:196–209, 2024.